Ocean, land, and atmosphere (OLA): a simple climate emulator for net-zero emission scenarios[*]

Aryan Eftekhari[†] Pratyuksh Bansal[‡] Doris Folini[§] Felix Kübler[¶]

Aleksandra Malova[‖] Simon Scheidegger[**] Olaf Schenk[††]

April 19, 2023

Abstract

We extend DICE-2016 with another time scale
Wish list:

- Extreme econ cases to confront with different carbon cycles

Keywords: climate change, social cost of carbon, carbon taxes, environmental policy, deep learning, integrated assessment models, DICE-2016

JEL classification: C61, E27, Q5, Q51, Q54, Q58

[*]We thank ..., as well as seminar participants at the University of Lausanne and the University of Zurich for very useful conversations and comments. This work was supported by the Swiss National Science Foundation (SNF), under project ID "Can Economic Policy Mitigate Climate-Change?", and for research support. Simon Scheidegger gratefully acknowledges support from the MIT Sloan School of Management.

[†]TBA, UNI; Email: bla.ch.

[‡]Institute of Computing, Università della Svizzera italiana; Email: pratyuksh.bansal@sam.math.ethz.ch.

[§]Institute for Atmospheric and Climate Science, ETHZ; Email: doris.folini@env.ethz.ch.

[¶]Department for Banking and Finance, University of Zürich; Swiss Finance Institute (SFI); Email: felix.kuebler@bf.uzh.ch.

[‖]Department of Economics, University of Lausanne; Email: aleksandra.malova@unil.ch.

[**]Department of Economics, University of Lausanne; Enterprise for Society (E4S); Email: simon.scheidegger@unil.ch

[††]Institute of Computing, Università della Svizzera italiana; Email: olaf.schenk@usi.ch.

1 Introduction

Suggested storyline:

- 1 paragraph blabla
- motivations of current paper: point out of current DICE (e.g., RCP)
- on an abstract level: 1 dynamic timescale missing.
- on a concrete level. We cannot resolve e.g. RCP2.6
- What are the economic implications: aggressive mitigation cannot be handled, etc...
- contribution from our side: go from 3 to 4 or 5 reservoirs.
- show how to calibrate it. Extend also test set by more tests (CDICE) to pin down the additional degrees of freedom.
- Contribution to climate science as stand-alone (preview of results): with this simple model(s), we show that we can correctly capture a),b),c), which contradicts the present opinion in the literature.
- from an econ applications point of view,

Climate modeling in the context of economic modeling consists, in essence, of translating carbon emissions generated by economic activity into atmospheric CO2 concentrations and on into a change in global mean temperature. Associated climate emulators (CEs) need to be computationally cheap, to free resources for the modeling of any none-climate aspects, yet 'fit for purpose [1]. The pivotal role of equilibrium climate sensitivity (ECS) when calculating the temperature change arising from an increase in atmospheric CO2 has long been recognized. A plausible reason why ECS has attracted so much attention from the economic community may be the uncertainty of ECS from a climate science point of view. Best estimates for ECS still range from roughly 2 to 4 degree Celsius, thus cannot be simply ignored in an economic context. Comparatively less attention is paid to uncertainties associated with the carbon-cycle, the second pillar of any climate model used in an economic context. Associated models vary in their level of complexity, ranging from simple impulse response function or two layer box models to more comprehensive models designed, for example, to account for hemispheric and depth dependent aspects of the oceans and to capture aspects of the land biosphere. The performance of one such model, a three-reservoir carbon-cycle model as used in the seminal DICE model, was assessed in some detail by Folini et al. (2022) from a climate science point of view and with regard to the impact of the carbon-cycle on economic aspects. It was demonstrated that i) a correct calibration of the carbon-cycle with respect to climate science bench marks is crucial and that ii) varying model calibration within bounds justified by climate science has a relevant impacts on economics, about half as big as from varying ECS (see Figure 12a in Folini et al. (2022)). The paper further stressed the relevance of the three-box carbon-cycle model featuring two response time scales, a fast and a slow one, in order to properly translate carbon emissions into atmospheric CO2 concentrations.

The present paper is a follow-up on Folini et al. (2022) in that it addresses the question of whether adding more carbon reservoirs has a relevant effect on the performance of the CE with regard to climate science and economics. We examine models consisting of three, four, or five carbon reservoirs that represent the atmosphere, the ocean, and possibly the biosphere on land. Addition of a land biosphere reservoir also paves the way to study climate mitigation scenarios explicitly involving the land biosphere for carbon capture and storage. The later question is of relevance in view of the Paris agreement and associated climate targets, like the 1.5 degree target. Climate science claims that reaching these goals implies a rapid decline in emission and even negative emissions later in this

[1]See Folini et al. (2022) for a more detailed discussion of what is meant by 'fit for purpose'.

century. The question arises whether simple carbon-cycle models as studied here are fit to purpose in view of such scenarios.

Mitigation scenarios distinguish themselves from business as usual scenarios in that carbon emissions decrease or even become negative (carbon sequestration) instead of steadily growing. From a carbon-cycle point of view this implies that partial pressure differences between notably the atmosphere and the ocean become smaller with time, as carbon emissions to the atmosphere diminish. With the difference in CO2 partial pressure between atmosphere and ocean diminishing, the uptake efficiency of the ocean decreases. Under extreme scenarios, the ocean may even turn from a CO2 sink to a CO2 source. Modeling of such behavior, of such re-distribution of carbon among reservoirs, necessitates that the entity of emitted carbon over time is still present in the model. This is the case for carbon-cycle box models, but not necessarily for impulse response function models. We quantify the capability of the simple box models at the heart of this study to successfully emulate this behavior, making the models suitable to study the connection between economy, strong mitigation scenarios, and climate.

We start from the functional form of the carbon-cycle as used in the widely used DICE-2016 model, a three-box model with one box for the atmosphere and two boxes for the ocean, one for the upper-ocean one for the deep-ocean. We add more reservoirs to the carbon-cycle model and follow the strategy outlined in Folini et al. (2022) to calibrate and bench mark the model. We note already here that additional bench marks specifically tailored to negative emissions or the land-biosphere reservoir do not form part of this study and are the topic of future work. Finally, we apply the newly calibrated carbon-cycle models to examine optimal abatement policies, focusing on whether the additional carbon-reservoirs make any difference in this resepect. The paper is organized as follows.

Things to stay before section 2

- Pre-industrial is assume do 1765
- Carbon REservoires at pre-industrial times are based on https://www.ipcc.ch/site/assets/uploads/2018/02/WG1AR5_Chapter06_FINAL.pdf
- Stability: Reduces variability in parameter estimates for different benchmark.
- short-time dynamics Salient
- Short-Term absorption discrepancy.

2 Climate Emulator

In this section, we will present our proposed methodology for a climate emulator, namely the carbon-cycle model, estimation procedure and calibration. We propose three carbon-cycle model configurations, which we categorized into two groups: serial and parallel. The models we considered include three reservoir classes: atmosphere (A), ocean (O), and land-biosphere (L). In the serial model, labeled as 3SR, the carbon cycle is modeled as three sequentially connected carbon reservoirs, with the atmosphere connected to the upper ocean O_1, and the ocean connected to the deep ocean O_2. In the parallel models, we introduced the land-biosphere, where carbon from the atmosphere is divided into two parallel streams: land-biosphere and ocean. The two parallel models are denoted as 4PR and 5PR. The 4PR model extends the 3SR model by adding a single land biosphere reservoir L_1, while the 5PR model (see, Figure 1 for visualization) splits the land biosphere reservoir into two sequential reservoirs associated with vegetation and soils, denoted as L_1 and L_2, respectively.

2.1 Carbon-Cycle

Let $\mathbf{m}^t \in \mathbb{R}^n$ be the amounts of carbon in p distinct reservoirs at discrete time steps $t = 1, 2, \ldots, T$. The carbon-cycle model can be characterized by the time-invariant operator $\mathbf{A} \in \mathbb{R}^{n\times n}$, which determines the rate of carbon mass exchange between these reservoirs. Accounting for emissions, denoted by $\mathbf{e}^t \in \mathbb{R}^n$, we describe the carbon-cycle using a first-order system of difference equations

$$\mathbf{m}^t - \mathbf{m}^{t-1} = h\mathbf{A}\mathbf{m}^t + \mathbf{e}^t, \tag{1}$$

where, h is the time-step size, and where $\mathbf{m}^0$ is the *initial condition*, which is known. The operator $\mathbf{A}$ possess real eigenvalues $-1 < \boldsymbol{\lambda}_i(\mathbf{A}) \leqslant 0$ for all i. For i and j, there exists a carbon transfer path between the reservoirs if $\mathbf{A}_{ij} \neq 0$, and there is no carbon transfer path if $\mathbf{A}_{ij} = 0$. Furthermore, $\mathbf{A}$ is restricted to satisfy both the *equilibrium condition* and the system *mass conservation*. The equilibrium conditions of the carbon-cycle are defined as

$$\mathbf{A}\mathbf{m}^{\mathrm{eq}} = \mathbf{0}, \tag{2}$$

where $\mathbf{m}^{\mathrm{eq}}$ denotes the equilibrium carbon masses, which is proportional to the eigenvector associated with the zero eigenvalue of $\mathbf{A}$. The principle of mass conservation is upheld by ensuring that

$$\mathbf{1}^\top(\mathbf{m}^t - \mathbf{m}^{t-1}) = \mathbf{e}^t \;\forall\, t \iff \mathbf{1}^\top\mathbf{A} = \mathbf{0}. \tag{3}$$

We define the *dynamic timescales* of the operator as $\boldsymbol{\tau}_i = 1/|\boldsymbol{\lambda}_i|$, excluding the zero eigenvalue, which corresponds to the infinite timescale associated with the equilibrium condition. Consequently, the potential dynamic timescales for the linear carbon-cycle model are $\boldsymbol{\tau}_i \in (1, \infty)$.

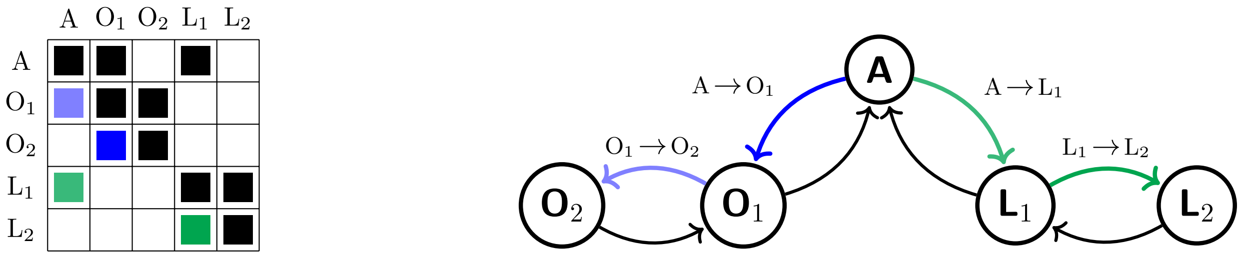

Figure 1: The operator $\mathbf{A}$ is visualized (left) for the 5PR model, which includes atmosphere (A), two ocean reservoirs(O_1 and O_2), and two land reservoirs (L_1 and L_2). A graphically representation of the connectivity of the reservoirs (right) is shown with the unknown carbon mass transfer rates denoted, for example, $O_1 \to O_2$ corresponds to the entry $\mathbf{A}_{3,2}$. The other model configuration 3SR and 4PR can all be considered as subsets of the more complex 5PR model configuration. $\mathbf{A}$ is symmetric in its non-zero pattern, but not in its values.

Configuration	Equilibrium Masses (GtC)				
	$\mathbf{m}_{\mathrm{A}}^{\mathrm{eq}}$	$\mathbf{m}_{\mathrm{O}_1}^{\mathrm{eq}}$	$\mathbf{m}_{\mathrm{O}_2}^{\mathrm{eq}}$	$\mathbf{m}_{\mathrm{L}_1}^{\mathrm{eq}}$	$\mathbf{m}_{\mathrm{L}_2}^{\mathrm{eq}}$
3SR	589	900	37,100	-	-
4PR	589	900	37,100	2,500	-
5PR	589	900	37,100	550	1,950

Table 1: Equilibrium masses in the different carbon reservoirs are shown for each configuration. For all configurations, O_1 and O_2 represent the upper and lower-ocean, respectively. In the 4PR model, L_1 denotes the total land-biosphere equilibrium mass, while the 5PR configuration subdivides the land-biosphere into vegetation L_1 and soils L_2. These masses correspond to the 1765 conditions, when the Earth's carbon cycle is assumed to be at equilibrium (for details, refer to Ciais et al. (2013) and the references therein).

Denote the nonzero strictly lower-triangular indices of $\mathbf{A}$ as $\mathcal{I} = \{(i, j) : \mathbf{A}_{ij} \neq 0, i > j\}$. For all model configurations outlined, applying conditions in (2) and (3), the closed-form solutions for the upper triangular values of the restricted operator are

$$\mathbf{A}_{ji} = \mathbf{A}_{ij} \frac{\mathbf{m}_j^{\mathrm{eq}}}{\mathbf{m}_i^{\mathrm{eq}}} \;\forall\, (i, j) \in \mathcal{I}, \text{ and } \mathbf{A}_{ii} = - \sum_{j=1, j\neq i}^{p} \mathbf{A}_{ij}. \tag{4}$$

The unknown parameters necessary for defining the restricted operator include the strictly lower triangular nonzero values $\mathbf{A}_{ij}$ for all $(i, j) \in \mathcal{I}$ and the ratios of the equilibrium masses $\mathbf{m}^{\mathrm{eq}}$. For a predefined sequence of emissions we denote the carbon-cycle simulation of length T as

$$\mathbf{M}[\mathbf{A}] := [\mathbf{m}^1, \mathbf{m}^2, \ldots, \mathbf{m}^T], \tag{5}$$

where $\mathbf{m}^t$ is defined as per (1). We utilize acronyms depicted in Figure 1 to refer to specific reservoirs; for instance, $\mathbf{M}[\mathbf{A}]^t_{\mathrm{O}_2}$ represents the content of the O_2 reservoir at time t. Throughout this work, our simulations are exclusively use atmospheric emissions, meaning e^t_{A} is non-zero only when emissions are present at time t, while all other entries are zero. Notice that only the ratios of $\mathbf{m}^{\mathrm{eq}}$ are relevant in the definition of $\mathbf{A}$. It is important to note that in defining $\mathbf{A}$, only the ratios of $\mathbf{m}^{\mathrm{eq}}$ are relevant. By simplifying the problem and setting $\mathbf{m}^{\mathrm{eq}}$ to the preindustrial values found in Table 1 (see, e.g., Ciais et al. (2013) and reference therein for further details), we reduce the unknown parameters to the non-zero values in the strictly lower-triangular matrix $\mathbf{A}$ (as seen in Figure 1). For the given model configurations, this corresponds to $n-1$ parameters. The time-stepping scheme using for the simulation is explicit Euler. [say more about stablity]

2.2 Estimation Procedure

Our proposed estimation procedure optimizes the $n - 1$ parameters of $\mathbf{A}$ by (1) minimizing the discrepancy between the our simulations and publicly available benchmarks,[2] while (2) penalizing solutions that do not conform to observed physical principles. The adopted simulation benchmarks are based on the work of Joos et al. (2013), in which various Earth System Models were used to simulate the decay of a 100 GtC pulse introduced into the atmosphere during preindustrial times when the Earth's carbon-cycle is assumed to be at equilibrium. Figure 2 showcases the benchmark dataset for the various models. We enforce three physical principles: (i) reducing variability in parameter estimates, (ii) minimizing dynamic timescales, and (iii) ensuring an approximately equal cumulative pulse emission flux from the atmosphere to both ocean and land biosphere reservoirs shortly after the pulse. We first begin with formalizing these physical principals, encoding them in in three district penalty functions q_1, q_2 and q_3. Subsequently, we outline the comprehensive optimization process for the estimation procedure.

[more text here]

[2]see, https://climatehomes.unibe.ch/~joos/IRF_Intercomparison/results.html for details

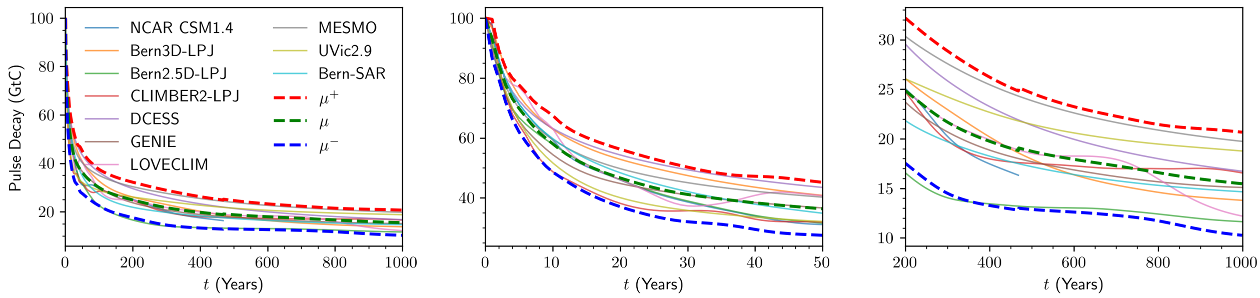

Figure 2: The decay of a 100 GtC pulse of emissions in the pre-industrial atmosphere (1765) was analyzed using various Earth System Models of differing complexities. This data is based on a series of controlled simulations conducted by Joos et al. (2013). For further details on the simulations and model descriptions, we refer the reader to the cited reference. The multi-modal mean of the simulations, denoted by μ, along with the two standard deviations above and below the mean, are represented by μ^+ and μ^-, respectively.

We employ three scenarios to estimate the operator parameters: the multi-modal mean and two standard deviation extrema, denoted as $\mathcal{B} := \{\mu, \mu^+, \mu^-\}$, respectively (see Figure 2 for details). Given a benchmark $b \in \mathcal{B}$, we obtain varying estimates of $\mathbf{A}^b$ for each b. The operator estimate $\mathbf{A}^b$ should be stable in the sense that the estimated parameters across the benchmarks should have similar values. To reduce the variability amongst the estimates $\mathbf{A}^b$, we penalize the difference between the parameter estimates with respect to $b = \mu$. We encode this attribute in the penalty function

$$q_1(\mathbf{A}^b) := \left\|\mathbf{a}^\mu - \mathbf{a}^b\right\|_2, \text{ where } \mathbf{a}^b := \{\mathbf{A}^b_{ij} : \forall (i,j) \in \mathcal{I}\}, \tag{6}$$

This penalty function results in a non-separable dependency between the parameter estimates. This dependency plays a critical role in constraining the range of potential operators that best fit the decay of atmospheric pulse emissions (see, e.g., Section X for further details.)

The proposed carbon-cycle model, along with various configurations, is a simplified approximation of a considerably more complex system. Rather than attempting to model processes across the spectrum of timescales, our goal here is to model the salient responses that play a significant role in the shortest timescales. To penalize large dynamic timescales we encourage increasing eigenvalues magnitudes of $\mathbf{A}^b$, which corresponds to the penalty function

$$q_1(\mathbf{A}^b) := \frac{1}{n}\mathrm{tr}(\mathbf{A}^b) = \frac{1}{n}\sum_{i=1}^{n} \boldsymbol{\lambda}_i(\mathbf{A}^b). \tag{7}$$

Since the eigenvalues of the operator are strictly real and non-positive, the corresponding penalty function is strictly non-positive. This approach is further motivated by the economic model (see Section X), in which long-term damages hold little significance due to the discounting factor.

Following the pulse event, it is expected that the total pulse flux will be equally distributed between the ocean and land reservoirs in the short term. This assumption is corroborated by Joos et al. (2013), where the simulation of a 100 GtC atmospheric emission (during preindustrial times) leads to an approximately equal partition of 60 GtC of cumulative emissions in the ocean and land carbon reservoirs within 40 to 60 years after the pulse. We incorporate this observation by limiting the cumulative flux discrepancy between the ocean and land reservoirs using the penalty function

$$q_3(\mathbf{A}^b) := \left\|\frac{\mathbf{M}^{t_e}_{\mathrm{O}}[\mathbf{A}^b] - \mathbf{M}^{t_e}_{\mathrm{L}}[\mathbf{A}^b]}{\mathbf{M}^{t_e}_{\mathrm{O}}[\mathbf{A}^b] + \mathbf{M}^{t_e}_{\mathrm{L}}[\mathbf{A}^b]}\right\|_2, \tag{8}$$

where $\mathbf{M}^{t_e}_{\mathrm{O}}[\mathbf{A}^b]$ is the total mass of all ocean reservoirs (and similarly, the superscript L denotes all land biosphere reservoirs) at time t_e. In our experiments, we set $t_e = 50$.

Let $\mathbf{y}^b$ represent the benchmark dataset of atmospheric carbon mass for the decaying 100 GtC pulse, spanning a total of T years after the pulse. In this pulse scenario, the emissions are defined as $\mathbf{e}_{\mathrm{A}}^1 = 100$ and zero for all other cases. Moreover, since we begin with preindustrial conditions, it follows that $\mathbf{m}^0 = \mathbf{m}^{\mathrm{eq}}$. Given the non-negative tuning coefficients ρ_1, ρ_2, and ρ_3, which correspond to each penalty function, the proposed estimation procedure seeks optimize

$$\min_{\{\mathbf{A}^b_b\}\,\forall\, b\in\mathcal{B}} \left\{ \sum_{v\in\mathcal{B}} \frac{1}{T} \left\| \mathbf{M}_{\mathrm{A}}[\mathbf{A}^b] - \mathbf{y}^b \right\|_2 + \rho_1 q_1(\mathbf{A}^b, \mathbf{A}^\mu) + \rho_1 q_2(\mathbf{A}^b) + \rho_3 q_3(\mathbf{A}^b) \right\}, \tag{9}$$

where $\mathbf{M}_{\mathrm{A}}[\mathbf{A}^b]$ represents the simulated values of atmospheric carbon content for the time period ranging from $t = 1$ to T.

[Say more about optimization method used ... and bounds of optimizer. The max percentage transfer of mass form one reservoir to the next is 15%]

2.3 Calibration

Configuration	Mass Flow Coefficients (Expressed as %)			
	$\mathbf{A}_{21}/\mathrm{A}\to\mathrm{O}_1$	$\mathbf{A}_{32}/\mathrm{O}_1\to\mathrm{O}_2$	$\mathbf{A}_{41}/\mathrm{A}\to\mathrm{L}_1$	$\mathbf{A}_{54}/\mathrm{L}_1\to\mathrm{L}_2$
3SR	15.00—14.98—14.99	0.14—0.22—0.37		
4PR	2.17—0.81—2.57	0.05—0.04—0.11	0.15—0.74—1.81	
5PR	0.4—0.85—2.41	0.05—0.04—0.11	0.41—0.91—2.52	12.96 13.21—12.98

Table 2: The umbers here are presented as % (ie, they should be divided by 100). The number follow the format (μ^+, μ, μ^-)

3 Simulation

3.1 Synthetic Scenarios

3.2 CMIP

3.3 MacDougall

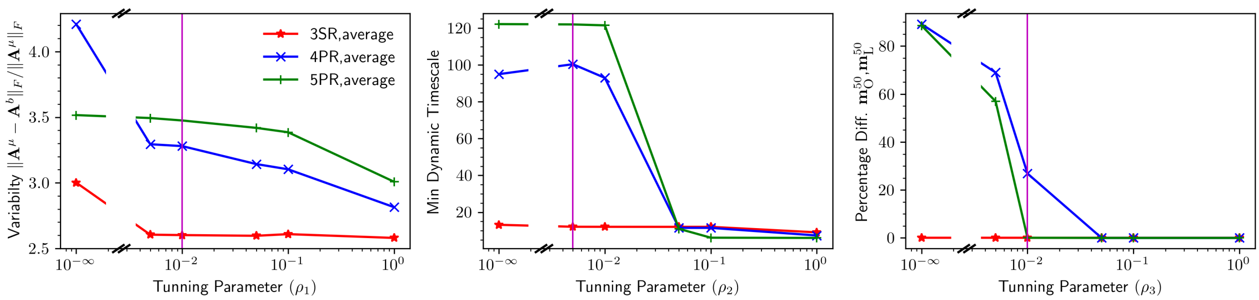

Figure 3: Objective Value Components (penalties)

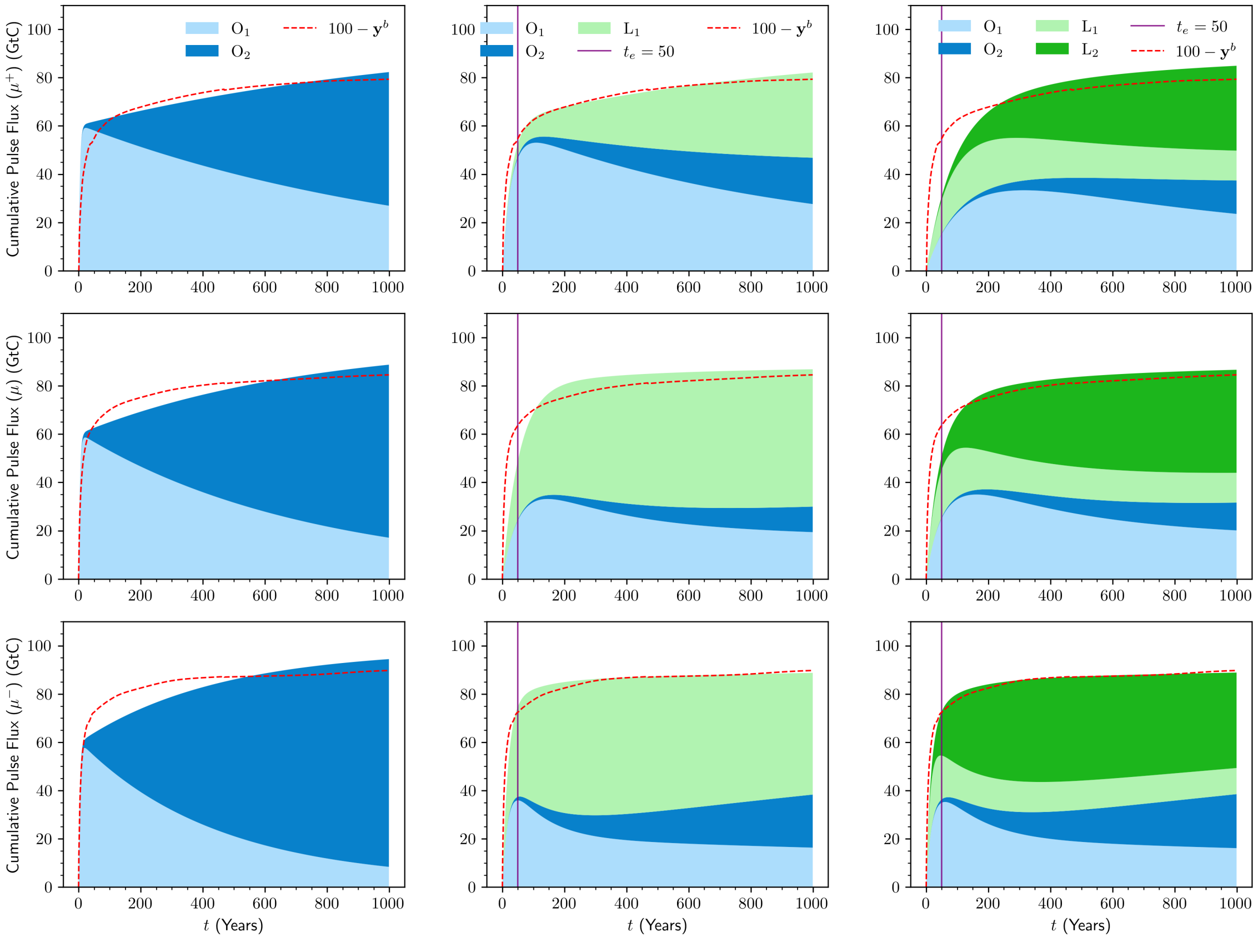

Figure 4: Pulse Cumulative FLux per model

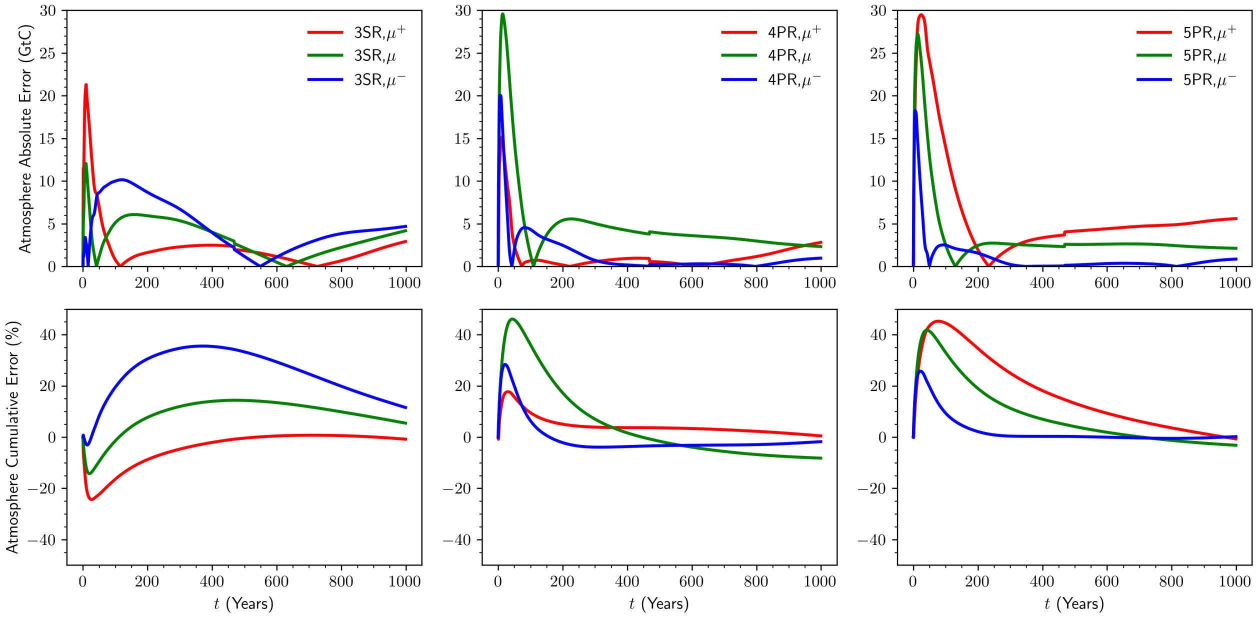

Figure 5: Pulse Fit Error

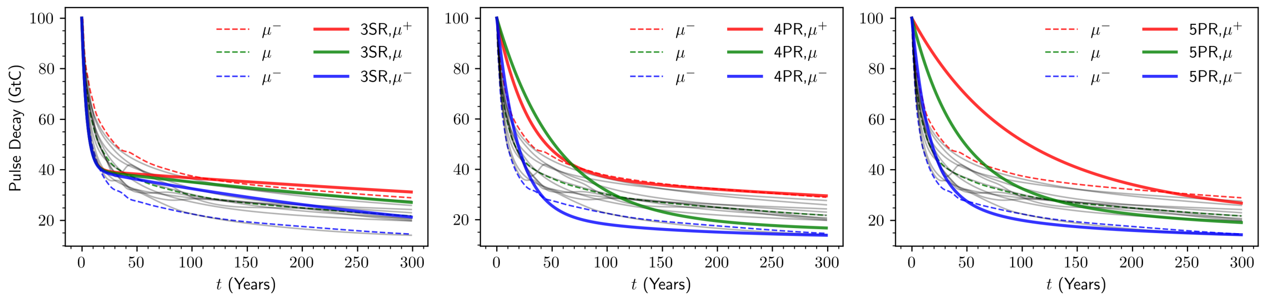

Figure 6: Joos 100 GtC Pulse (symmetry of the response to a negative pulse given due to linearity of the model)

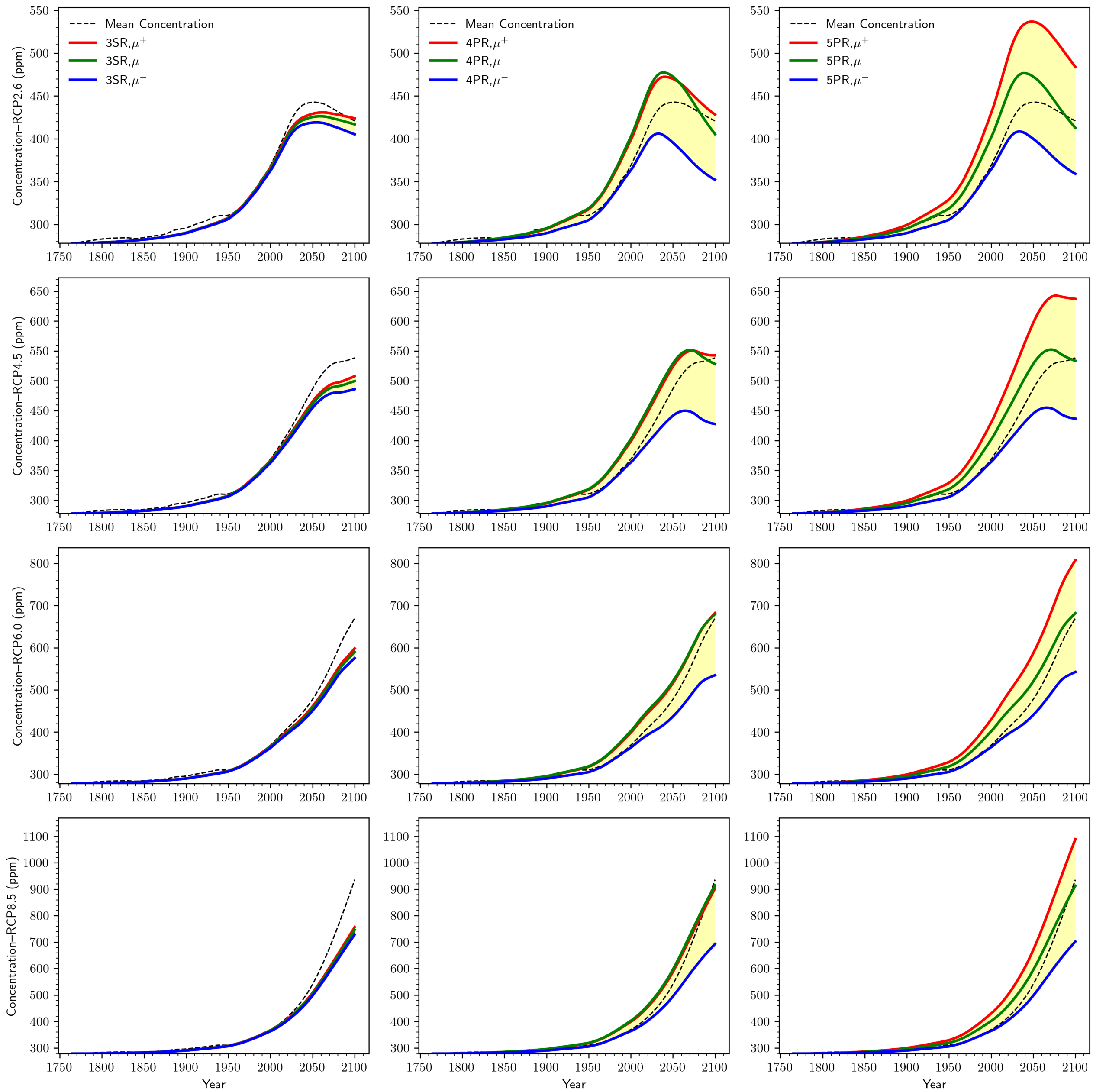

Figure 7: CMIP Concentrations

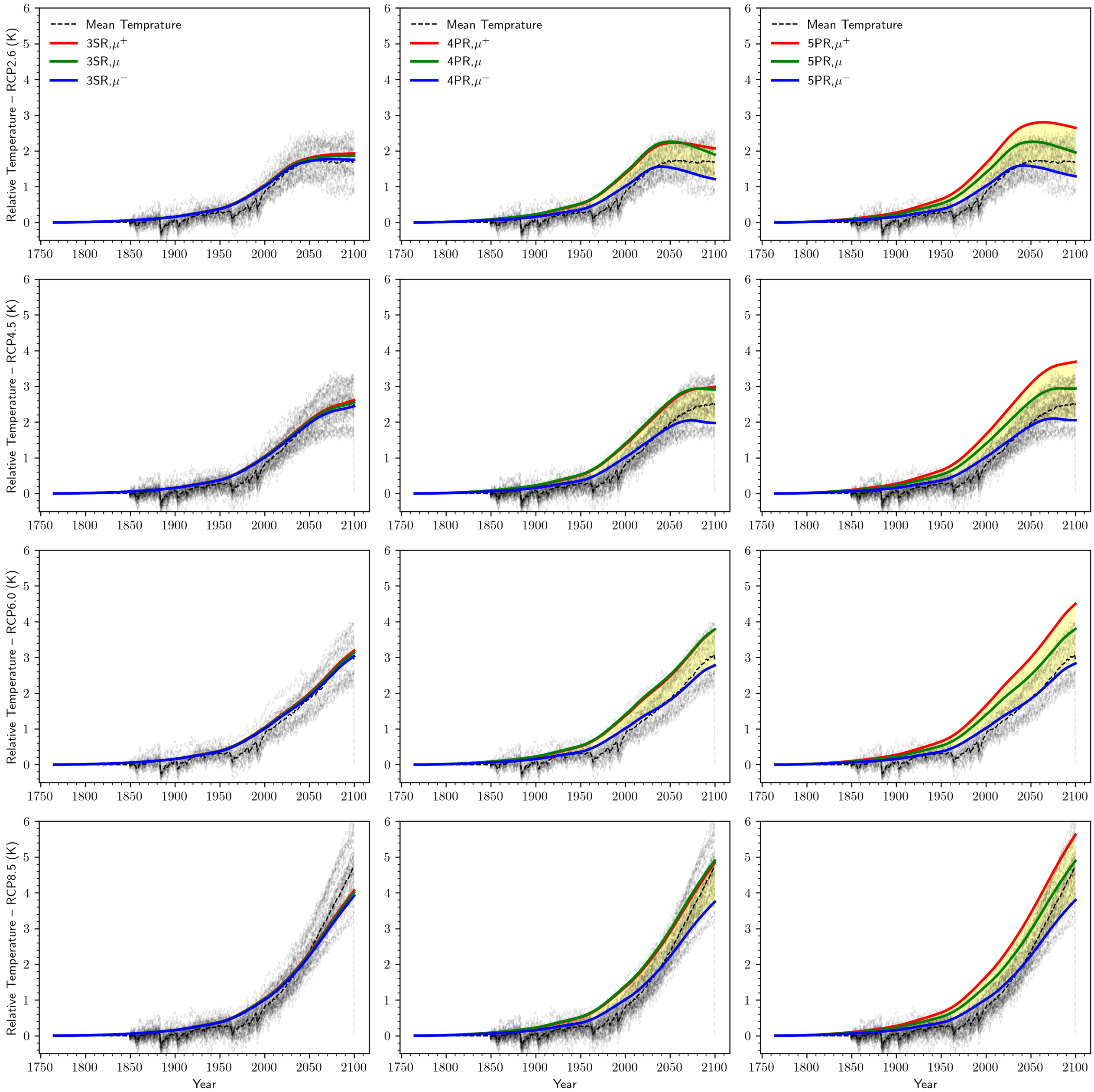

Figure 8: CMIP Temprature

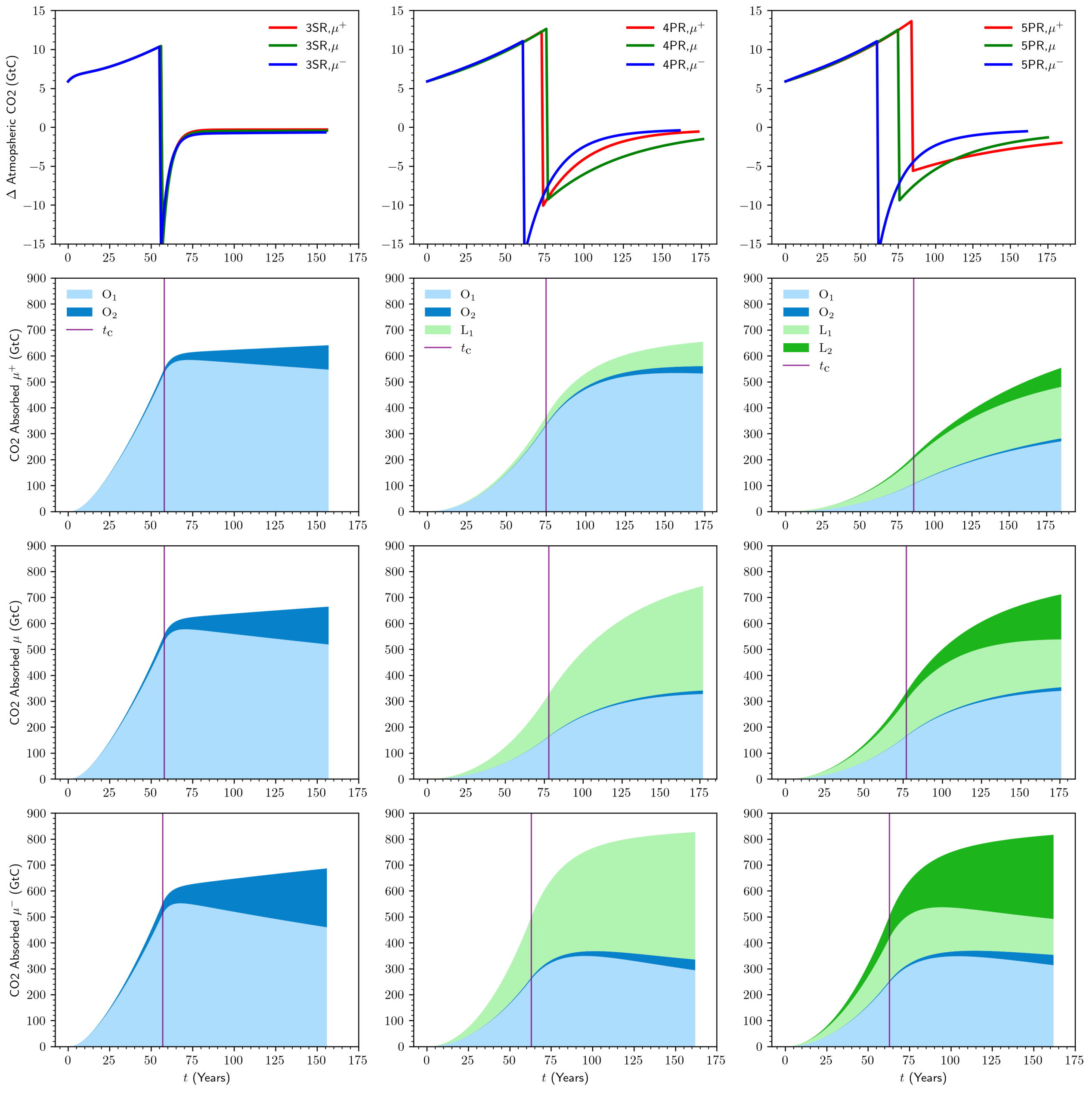

Figure 9: MacDougall 1, Note t_c is the time at which the emission of MacDougall end and the system is left to "coast".

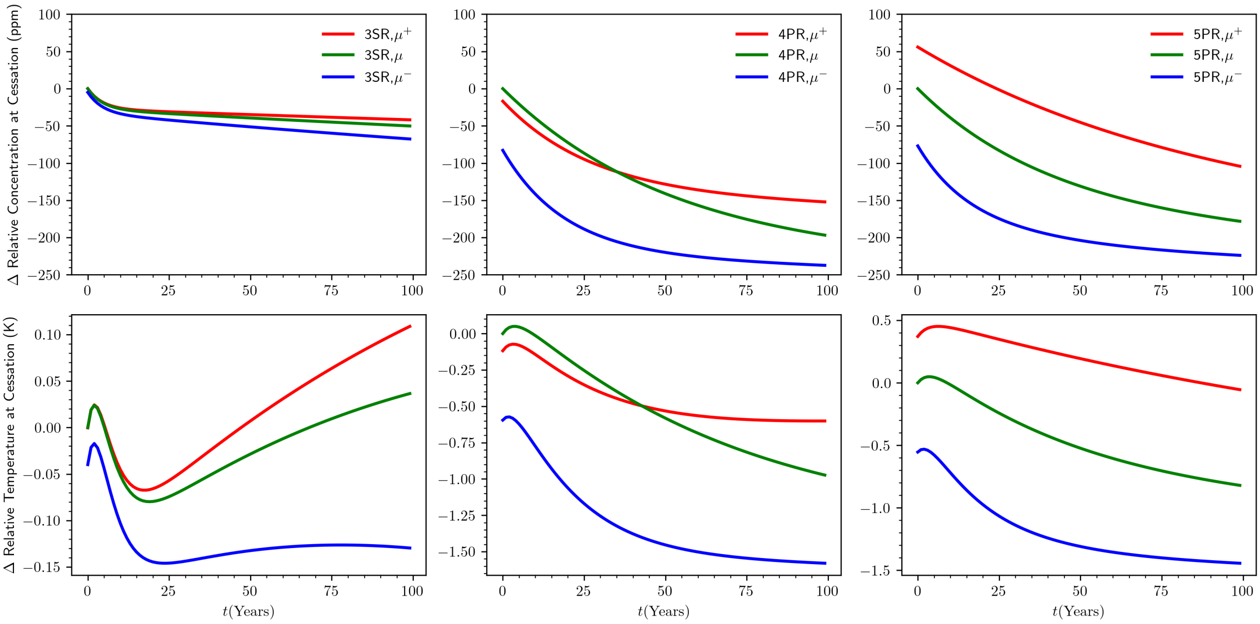

Figure 10: MacDougall 2: System response after emission have stopped.

Bibliographies

Ciais, P., C. Sabine, G. Bala, and W. Peters. 2013. Carbon and Other Biogeochemical Cycles. Cambridge University Press, 465–570. Complete rapport op http://www.climatechange2013.org/report/.

Joos, Fortunat, Raphael Roth, Jan S Fuglestvedt, Glen P Peters, Ian G Enting, W von Bloh, Victor Brovkin, Eleanor J Burke, Michael Eby, Neil R Edwards et al. 2013. "Carbon dioxide and climate impulse response functions for the computation of greenhouse gas metrics: a multi-model analysis." Atmospheric Chemistry and Physics 13 (5):2793–2825.